Modeling of roughness evolution during the etching of inhomogeneous films: Material-induced anomalous scaling

V. Constantoudis,* H. Christoyianni, E. Zakka, and E. Gogolides
Institute of Microelectronics, NCSR "Demokritos", Aghia Paraskevi, Athens 15310, Greece
(Received 16 December 2008; published 23 April 2009)

Although a lot of experimental and model results for roughness evolution exhibit anomalous scaling, the origins of such a behavior remain still unclear. In this paper, the possible contribution of material inhomogeneities to the appearance of anomalous scaling behavior in kinetic roughening is investigated by a simple modeling of roughness evolution in the etching of porous and composite films. It is found that the roughness evolution during the etching of both kinds of inhomogeneous films displays anomalous scaling behavior with peculiar features (no expansion of correlations vs time and square-root time increase in surface width roughness) defining a new universality class. Furthermore, the insertion of correlations between film pores or fillers along etching direction leads to roughness instability, i.e., linear increase in surface width roughness. The latter observation may be exploited for the detection of correlations between pores or fillers using roughness evolution as a diagnostic tool.

DOI: 10.1103/PhysRevE.79.041604 PACS number(s): 81.15.Aa, 68.35.Ct, 89.75.Da, 81.65.Cf

I. INTRODUCTION

The investigation of the formation and evolution of surface roughness during the etching of a film (open area or patterned) has both theoretical and technological motivations. Theoretically, roughness evolution is a typical example of complex nonequilibrium statistical process taking place in both space and time regimes, which, due to the lack of a well-established theory for nonequilibrium processes, challenges theoreticians to test new or to modify older concepts and methods for its characterization, understanding, and control. Last decades, a large amount of works devoted to the transfer of methods and concepts from the statistical mechanics of critical phenomena (scaling exponents, universality classes, etc.) to the description of roughness evolution renewing the theoretical interest [1–3]. The technological motivation comes from the recent strong trend in technology toward the fabrication of devices with features on micrometer and even nanometer scales (microtechnology and nanotechnology). At these scales, the surfaces of the features cannot be considered smooth since their roughness, usually at the same scale, starts to affect device performance. In order to reduce and/or control these effects further investigation and understanding of roughness formation and control are required.

One of the most widely used tools for the patterning of films and fabrication of device features is their selective etching using either wet etchants or dry plasma gases or ion beams. Etching has been applied with great success on microscale patterning and now is aiming to be extended to nanoscale regime. It is considered with lithography as the driving horses of the top-down approach to nanotechnology. A critical issue for its continuing success on nanoscale is the control of roughness it induces on fabricated surfaces. The importance of this issue increases when the films to be etched are inhomogeneous (i.e., the local etch rate varies in the bulk material). Inhomogeneous films may be films of either porous or composite material. To give an example, it has been measured that the roughness of a Si film after etching 50 000 nm is only 7 nm, whereas the etching of only 500 nm of a inhomogeneous film (GaSb) induces 30 nm surface roughness [4,5]. This fact in combination with the increasing technological relevance of inhomogeneous and composite materials in many fields due to their beneficial properties emphasizes the need for further investigation of roughness formation and evolution during the etching of inhomogeneous films.

A simplified schematic of this formation is shown in Fig. 1. An initially flat film with inhomogeneities inside it (blank circles) is etched in an appropriate environment and becomes rough. Obviously, the formatted roughness depends on three factors. The first is the nature and characteristics of the etchants, the second is the interactions of the etchants with the surface atoms and molecules, and the third is the bulk structure of the material and its reaction to the etching process. The contribution of the first two factors especially in homogeneous films has been studied widely [6–14], whereas the third one, crucial in inhomogeneous etching, has been considered only in a limited number of publications [15–18].

The aim of the present paper is to contribute to the investigation of the effects of film inhomogeneities to surface roughness formation and evolution by a simple modeling approach. The key idea is to simplify the etching process as

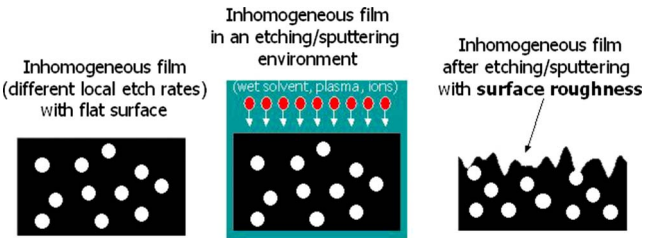

FIG. 1. (Color online) Schematic representation of roughness formation on the surface of an initially flat inhomogeneous film caused by etching or sputtering.

*vconst@imel.demokritos.gr

much as possible, so that the impact of the etched material inhomogeneities on roughness evolution is clearly revealed.

More specifically the focus is on the spatiotemporal scaling behavior of roughness evolution during etching. Recently, it has been found that a large number of experimental and modeling roughness evolutions do not follow the normal scaling behavior proposed by Family and Viscek [19] but exhibit anomalous scaling behavior demanding new scaling exponents and relationships among them [18,20–23]. The main question posed in this paper is what type of scaling behavior (normal or anomalous) the material inhomogeneities tend to induce on surface roughness evolution during etching. Moreover, the impact of the correlation of inhomogeneities as well as their geometric characteristics on roughness evolution is investigated. Both films of porous materials and composites with fillers having lower etching rate than bulk material will be modeled and etched by the simple model mechanism.

The structure of the paper is as follows. In Sec. II a brief account of some theoretical definitions and information on static and kinetic roughness will be given for the sake of completeness. Then, Sec. III describes the simple model etching mechanism as well as the representation of etched films. The results of this modeling approach for porous and composite materials will be presented in Secs. IV and V, respectively. Finally, Sec. VI summarizes the main results of the paper.

II. BRIEF ACCOUNT ON STATIC AND KINETIC ROUGHNESS THEORY

Surface roughness is the deviation from flatness and, actually, is a spatiotemporal complex phenomenon whose time evolution depends on spatial distribution and vice versa. To make the presentation of its basic characteristics as clear as possible, one can distinguish two aspects of roughness: static and kinetic. By static roughness we mean the roughness at a specific moment of time ignoring its time dependence (evolution), whereas when time evolution is on the focus, we speak about kinetic roughness.

A. Static roughness

Static roughness in two or three dimensions can be characterized by many parameters and functions. One of the most commonly used is one member of correlation functions, the height-height correlation function (HHCF) $G(r)$ [1,24]. For a one-dimensional (1D) surface $h(x)$, it is defined as

$$G(r) = \sqrt{\langle [h(x+r) - h(x)]^2 \rangle}, \tag{1}$$

where $\langle \cdots \rangle$ denotes averaging over the whole surface. The definition can be easily extended to two-dimensional (2D) surfaces but it is not written here since, in this paper, we are limited to 1D surface evolution.

A typical form of the HHCF of a rough surface is shown in Fig. 2. As we can see, this is characterized at low r by a power-law increase $[G(r) \sim r^{\alpha}]$ followed by a saturation above a critical distance $r \sim \xi$ to a value $G(r \to \infty)$. The power-law increase reveals the fractal (self-affine) symmetry

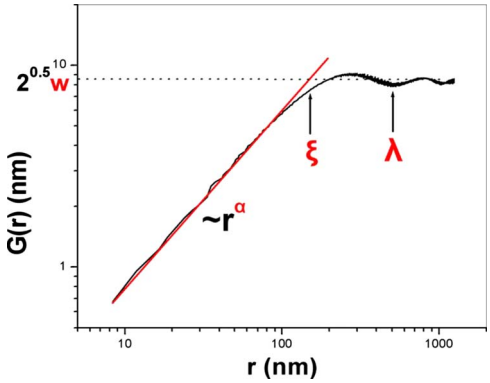

FIG. 2. (Color online) A typical example of the height-height correlation function $G(r)$ of a rough surface with periodicity. Notice the relationship of its form with the roughness parameters w, α, ξ, λ.

quantified by the exponent α called roughness exponent, which is related to the fractal (box counting) dimension of the surface since $\alpha = 2 - d$ [1]. The fractal self-affine symmetry is limited to scales lower than the critical distance ξ, which is related to the correlation length of the surface. For distances larger than ξ, the surface points can be considered uncorrelated. The saturation value is related to the surface width w of the surface points through the relation $G(r \to \infty) = \sqrt{2}w$. In case of periodic fluctuations on surface, a persistent oscillation of HHCF for $r > \xi$ appears whose first minimum (λ in Fig. 2) corresponds to the apparent wavelength of the periodic fluctuations.

The above example shows that a typical rough surface with scale-limited fractality can be characterized by three parameters: surface width w, roughness exponent α, and correlation length ξ. In case of periodicity, the wavelength λ should be added along with the system correlation length, which indicates the distance at which periodicity is extended.

B. Kinetic roughness

The term kinetic roughness has been coined for the description of the time evolution of roughness fluctuations. According to the behavior of the local and global surface fluctuations vs treatment time, kinetic roughness can exhibit normal or anomalous scaling behavior [2,3,25].

1. Normal kinetic roughness

In normal kinetic roughness, the surface width w is independent of the processing time t, for small values of the surface length L or equivalently the height-height correlation function $G(r)$ is independent of the time t at small distances r [Fig. 3(a)]. Figure 3(b) shows a typical example of 1D surface evolution exhibiting normal kinetic roughness. The roughness exponent α characterizes the spatial roughness morphology: $w(L) \sim L^{\alpha}$ for $L < \xi_w$ ($\propto \xi$) and the growth exponent β quantifies the time dependence of surface width: $w(t) \sim t^{\beta}$ for $t < t_c$. The dynamic exponent z is defined through the time dependence of spatial correlations quantifying by the correlation length: $\xi \sim t^{1/z}$.

The spatiotemporal behavior of roughness in normal kinetic roughness can be summarized in the Family-Viscek dynamic scaling relation [19]

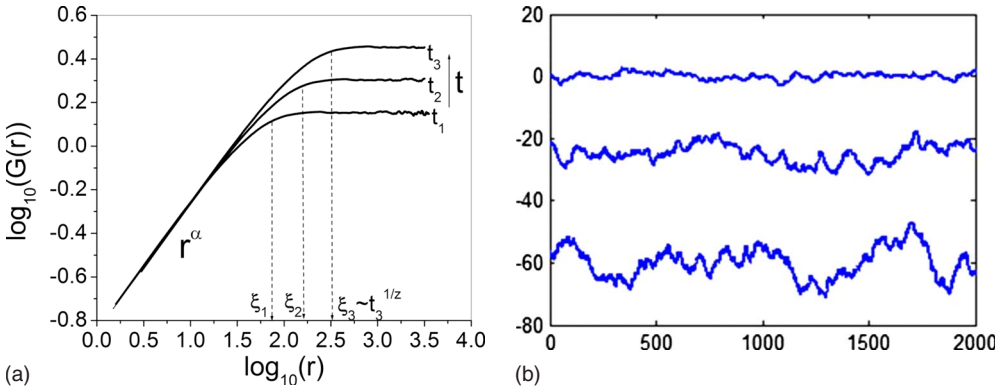

FIG. 3. (Color online) (a) Time dependence of height-height correlation function $G(r)$ and (b) 1D surface morphology evolution in normal kinetic roughness. Notice the symmetric at all scales development of roughness vs time.

$$w(L,t) \sim t^{\beta} f[L/\xi(t)] \tag{2}$$

with $f(u) \sim u^{\alpha}$ if $u \ll 1$, i.e., $w(L,t) \sim L^{\alpha}$ for $L \ll \xi(t) \sim t^{1/z}$ and $f(u) \sim$ const if $u \gg 1$, i.e., $w(L,t) \sim t^{\beta}$ for $L \gg \xi(t)$. The extraction of the above equations assumes that the three scaling parameters α, β, and z are not independent and satisfy the relation $z = \frac{\alpha}{\beta}$.

2. Anomalous kinetic roughness

In anomalous kinetic roughness, w depends on the etching time t even at small line lengths L. This differentiation from the Family-Viscek behavior is due to the presence of local surface fluctuations which are enhanced with time and result in the increase in $w(L)$ for small L or $G(r)$ at low r, as shown in Figs. 4(a) and 4(b) [3,18,20–24]. Therefore, we need a new more general scaling relation capable of differentiating local from global roughness behavior.

This relation is the general anomalous dynamic scaling ansatz [20],

$$w(L,t) \sim t^{\beta} f_A[L/\xi(t)] \tag{3}$$

with $f_A(u) \sim u^{\alpha_{\mathrm{loc}}}$ if $u \ll 1$, i.e., $w(L,t) \sim t^{(\beta-\alpha_{\mathrm{loc}}/z)} L^{\alpha_{\mathrm{loc}}}$ for $L \ll \xi(t) \sim t^{1/z}$ and $f_A(u) \sim$ const if $u \gg 1$, i.e., $w(L,t) \sim t^{\beta}$ for $L \gg \xi(t)$. From the above equations we observe that, for $L < \xi$,

$$w(L,t) \sim t^{\beta^*} L^{\alpha_{\mathrm{loc}}}$$

with $\beta^* = \beta - \alpha_{\mathrm{loc}}/z$ as a new scaling parameter which determines the dependence of $w(t)$ at small L. When $\alpha_{\mathrm{loc}} = \alpha$, then surface roughness evolves smoothly following the Family-Viscek symmetry and local roughening mechanisms such as diffusion dominate. On the contrary, when $\alpha_{\mathrm{loc}} < 1$ and $\alpha_{\mathrm{loc}} < \alpha$, surface roughness exhibits anomalous behavior and nonlocal mechanisms such as shadowing govern roughness evolution.

III. MODELING METHODOLOGY

The modeling methodology includes the modeling of the etched film and etching process. For the film, we choose the cellular representation in which the film is considered as a 2D lattice of square cells. In porous films modeling, each void (pore) is represented by a number of empty cells forming the shape (circular, square, triangular, etc.) of the void. Void dimensions determine the number of the empty cells belonging to a void, while the total number of voids in film gives the free volume parameter V_{free}. The positions of the pores in film may be uncorrelated or with some kind of correlations. Not surprisingly, the most important pore correlations are those along the direction that etching proceeds (ver-

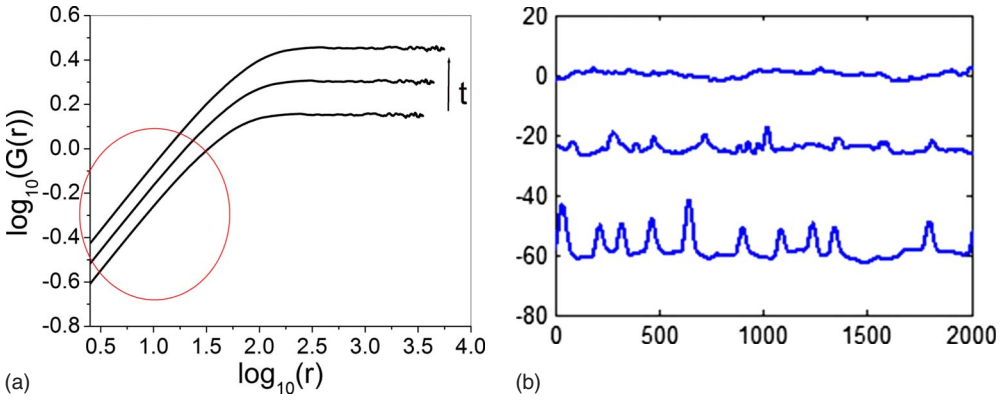

FIG. 4. (Color online) (a) Time dependence of height-height correlation function $G(r)$ and (b) 1D surface morphology evolution in anomalous kinetic roughness. Notice the anomalous enhancement of local fluctuations in the form of columns (in the figure) or holes, which result in the upward shift of $G(r)$ at small r shown within the circle.

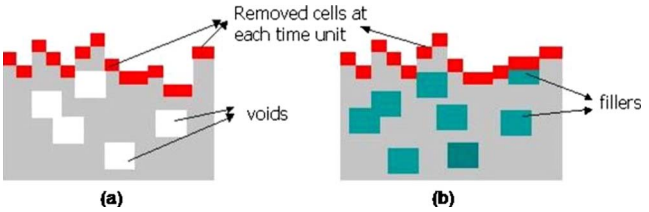

FIG. 5. (Color online) Schematic representation of layer by layer etching of (a) porous and (b) composite films.

tical dimension). Thus the input in the model consists of the following material parameters: (a) pore geometry (circles, rectangles, and triangles), (b) vertical and horizontal pore dimensions (R_y and R_x, respectively), (c) total free volume V_{free}, and (d) pore position vertical correlations.

In the case of composite films, the voids are replaced with fillers and the above input parameters properly modified still hold (for example, the total free volume V_{free} is replaced with the total filler volume V_{filler}). Furthermore, one more input material parameter should be added and this is the ratio of the etching rate of bulk material with respect to the etching rate of difficult to be etched fillers (etch filler selectivity s).

As regard the etching process, the key idea is to simplify it, so that material inhomogeneity effects on roughness evolution can be revealed more clearly. The simplest etching scheme, which can be considered, is the layer by layer removal of film cells [layer by layer etching (LLE)], which resembles the anisotropic etching but with no randomness. At each time unit, the top (surface) cell of each material column is removed. Figure 5 depicts schematically the LLE process. Obviously, in homogeneous films, LLE induces no roughness. Thus, the roughness appeared during the LLE of inhomogeneous films in total comes from film inhomogeneities quantified by the above-mentioned input parameters.

The output of the model includes the calculation of the surface width w and the HHCF $G(r)$ versus etching time measured at lattice units (l.u.). From these dependencies, we can extract the scaling critical exponents of spatiotemporal roughness evolution and decide the universality class that it may belong.

IV. LAYER BY LAYER ETCHING OF POROUS FILMS: MODELING RESULTS FOR ROUGHNESS EVOLUTION

A. Effects on $w(t)$

First we consider the LLE of a typical porous film with circular voids of fixed radius R positioned randomly (with no correlations) inside it [see Fig. 6(a)]. The time evolution $w(t)$ for such a film with $R=5$ and $V_{\text{free}}=0.1$ is given in Fig. 6(b). As we can see, for $t>t_{\text{cr}}$ w increases as the square root of time: $w(t)\sim t^{1/2}$. The critical time t_{cr} is found to be equal to the diameter of the circular pores ($t_{\text{cr}}\sim 2R$). Similar behavior in the time increase of w has been predicted and found when random removal of surface cells of a homogeneous film is considered [1] or in the LLE of a film with randomly distributed local etch rates [26]. It seems that any kind of uncorrelated randomness involved in the etching process contributes to square-root time increase of w.

The effects of free volume, pore dimensions, and geometry are expected to be contained alone in the prefactor f of the complete relation giving $w(t)$ as follows:

$$w(t) = f(R, V_{\text{free}}, \text{geometry}) t^{1/2}.$$

An approximated analytical formula for this prefactor f can be estimated in a heuristic semiempirical way and is given by

$$f(R, V_{\text{free}}, \text{geometry}) = \sqrt{2R \frac{V_{\text{free}}}{1 - V_{\text{free}}}}. \quad (4)$$

Figure 7 demonstrates the success of this simple formula in capturing the material parameters effects on w at a specific time moment ($t=800$) by depicting the numerical results with the predictions of Eq. (4) for various void radii R and free volumes V_{free}.

The generalization of this formula is straightforward and the general formula giving the time evolution $w(t)$ during the LLE of a porous film with randomly distributed voids of any geometry and dimensions is

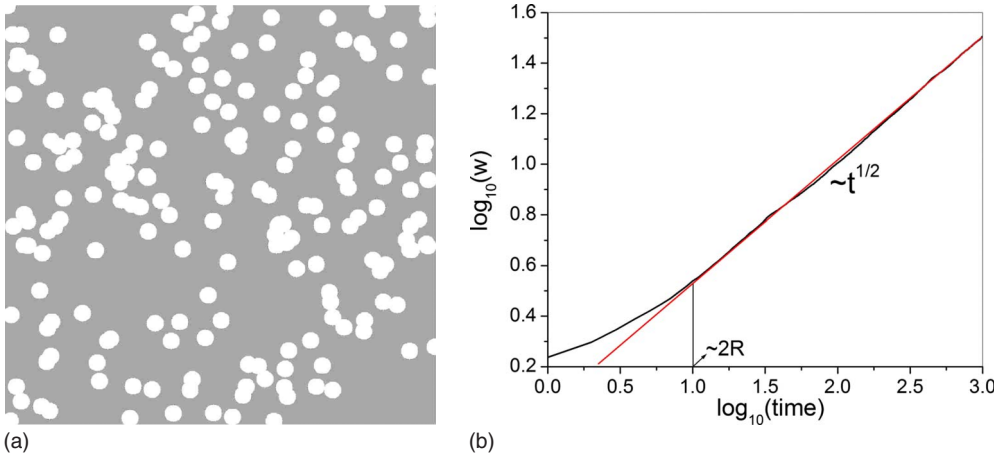

FIG. 6. (Color online) (a) 2D inhomogeneous film with circular pores of radius R randomly distributed in the bulk material and (b) the evolution of w with LLE time for $R=5$ and $V_{\text{free}}=10\%$. The square-root time law dependence is obtained after a transient behavior of slower roughening for $t<t_{\text{cr}}\sim 2R$.

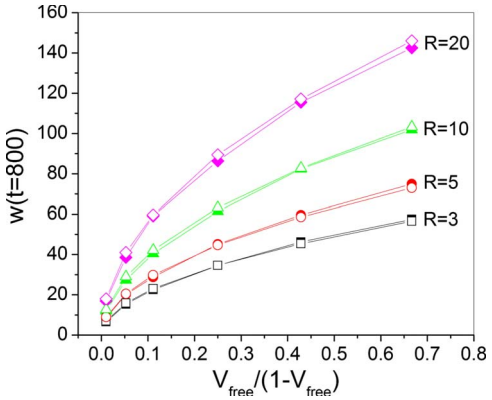

FIG. 7. (Color online) Comparison of numerical results (full symbols) for the dependence of $w(t=800)$ on V_{free} with the predictions of formula (4) (open symbols) for various radiuses of circular voids: $R=3$ (squares), $R=5$ (circles), $R=10$ (upper triangles), and $R=20$ (diamonds).

$$w(t) = \sqrt{R_y \frac{V_{\text{free}}}{1 - V_{\text{free}}} t}, \tag{5}$$

where R_y is the linear dimension of pores along etching direction. As we can clearly see, no effects of horizontal void dimensions or void geometry are included in time increase of w.

B. Effects on $G(r,t)$

In this section, the effects of material parameters on the evolution of spatial surface roughness aspects are reported. Figure 8 shows the HHCF $G(r)$ for various etching times and for two different void geometries: (a) circular and (b) rectangular.

From the form of $G(r)$ and their time dependence the following conclusions can be obtained:

(a) The LLE of inhomogeneous films induces on the etched surface fractal self-affine behavior in limited scale range revealed by the power-law increase at low r. The upper limit of this range is marked by the correlation length which in circular voids equals R and in rectangular corresponds to

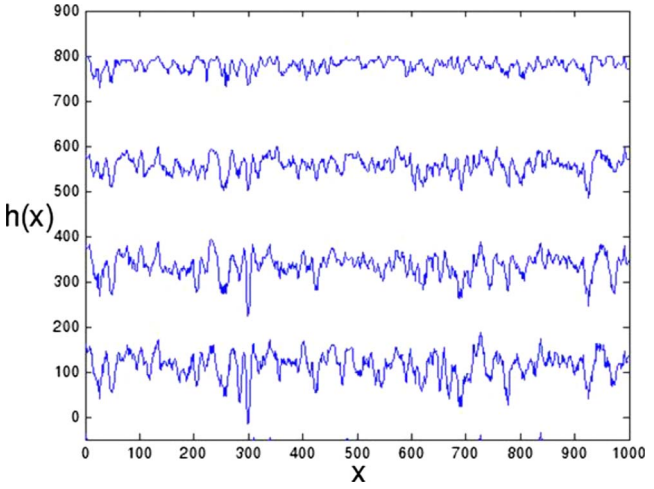

FIG. 9. (Color online) 1D surface evolution during the LLE of an inhomogeneous porous film with circular voids of $R=5$ and total free volume of 10%.

R_x. In the general case of voids with any shape, the correlation length is related to the horizontal dimension of voids, whereas the vertical void dimension affects the evolution of $w(t)$.

(b) The roughness exponent α is found to be affected by void geometry and is equal to 0.63 for the circular voids and 0.48 for rectangular ones. Thus, the only output parameter that seems sensitive to void shape changes is the roughness exponent α and therefore the surface fractal dimension.

(c) As regard the kinetic roughening behavior, the continuous increase in $G(r)$ at low r reveals the anomalous scaling behavior of roughness evolution. However, this behavior is not accompanied by the presence of peaks but by the gradual development of dips, as it demonstrated by Fig. 9 where the time evolution of a surface profile during LLE is shown. Furthermore, it is not related with roughness instability ($w \sim t$) but, quite surprisingly, with the milder square-root time increase ($w \sim t^{1/2}$). As we have seen in Sec. II, the anomalous kinetic roughening can be quantified by four critical scaling exponents: the growth exponent β, the roughness exponent α, the dynamic exponent z, and the exponent β'

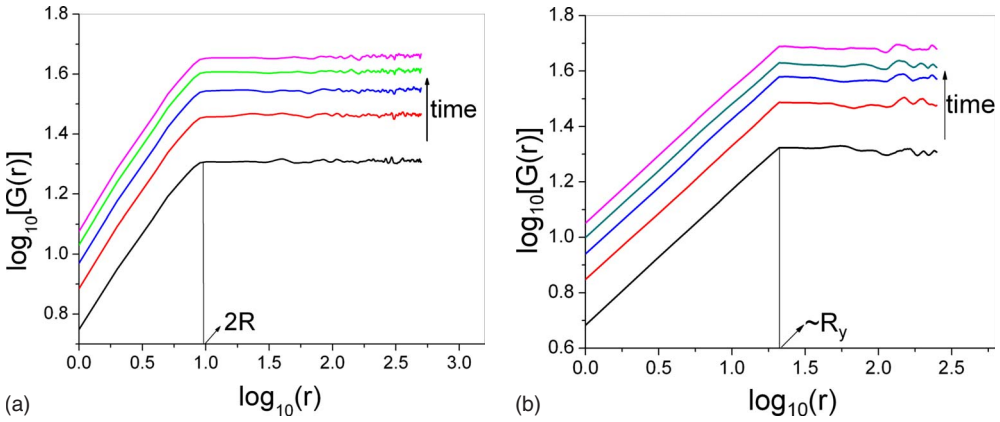

FIG. 8. (Color online) Time evolution of the HHCF $G(r)$ for two different void geometries: (a) circular (circular radius $R=5$) and (b) rectangular (rectangular dimensions $R_x=10$ and $R_y=20$).

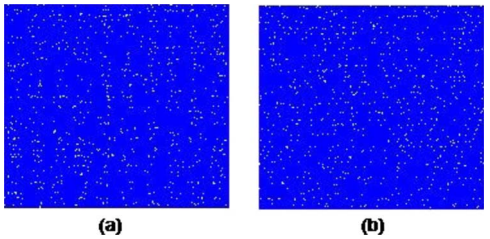

FIG. 10. (Color online) 2D films with the void centers in the case they are vertically (a) correlated or (b) uncorrelated.

giving the low-r $G(r)$ power-law increase $[G(r<\xi)\sim t^{\beta'}]$. These should be connected through the relation $\beta'=\beta-\alpha/z$.

The striking peculiarity of the roughness evolution shown in Fig. 8 is that the correlation length remains fixed during etching. This means that $z=\infty$. The parallel upward shift of $G(r)$ shows that both $G(r<\xi)$ and $G(r\gg\xi)$ scale with time in similar manner leading to the equality $\beta'=\beta$. Thus, independently on the value of the roughness exponent α, the anomalous scaling ansatz seems to hold in the LLE of porous films. Additionally, to the best of our knowledge this tetrad of critical scaling exponents ($\beta=\beta'=0.5$ and $z=\infty$ and any α) has not been observed in other cases of roughness evolution and thus defines another universality class.

C. Effects of pore position correlations along etching direction

In order to see the effects of pore position correlations on roughness evolution, we generate and employ pore films with correlated voids along the direction of etching (vertical direction). In these films, the density of voids along the horizontal direction exhibits an oscillatory variation, which is determined by the amplitude A and wavelength λ. The degree of vertical correlations is quantified by A. $A=0$ corresponds to isotropic distribution of pores with no correlations, whereas $A>0$ imposes correlations between pores along vertical direction which become stronger with A. Figure 10(a) shows the void centers of a film which are vertically correlated, while for the sake of comparison Fig. 10(b) displays a film with uncorrelated randomly distributed voids. Although the difference does not seem great, Fig. 11 demonstrates that it affects surface width increase $w(t)$ significantly. Indeed, Fig. 11 shows that the presence of even slight vertical correlations in void positions in the film induces roughness instability since it shifts the growth exponent β from 0.5 to 1. Thus, although growth exponent is irrelevant to changes in the number and dimensions of voids, it is found to be sensitive to the presence of slight correlations between void positions.

This sensitivity of roughness growth exponent to void correlations may open new prospects to roughness studies. Instead of being only the output of a process affecting the fabricated device, it can be thought as a diagnostic tool for the detection of void position correlations in the etched inhomogeneous film. Given the rapid advances in roughness metrology and the increasing technological importance of inhomogeneous films, we believe that this usage of roughness evolution will attract a lot of interests in the near future.

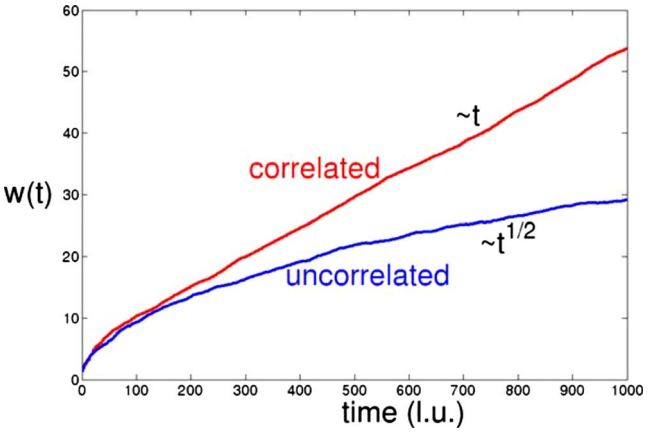

FIG. 11. (Color online) Surface width vs time $w(t)$ during LLE of inhomogeneous porous films with vertically correlated and uncorrelated positions. Notice the clear shift of the growth exponent from 0.5 to 1 when vertical correlations are taken into account.

V. LAYER BY LAYER ETCHING OF COMPOSITE FILMS: MODELING RESULTS FOR ROUGHNESS EVOLUTION

A. Effects on $w(t)$

A typical time evolution $w(t)$ during the LLE of a composite film is shown in Fig. 12. The dependencies of $w(t)$ on material parameters appear also in the same figure. As we can see, $w(t)$ for $t<t_{cr}$ is characterized by a transient behavior, during which w increases almost linearly with time. The critical time t_{cr} is much larger than that in porous films and equals to sR_y, where R_y is the vertical dimension of fillers in the film. After this time the etching may stop and consequently w remains fixed for a period which is proportional to V_{filler}. For small V_{filler}, this etch stopping does not appear. For longer times, w starts to increase again but now slower than for $t<t_{cr}$ following the square-root time law, which, as referred in Sec. IV, is typical for random roughening processes.

Thus, for long etch times, the roughness evolution obeys the formula

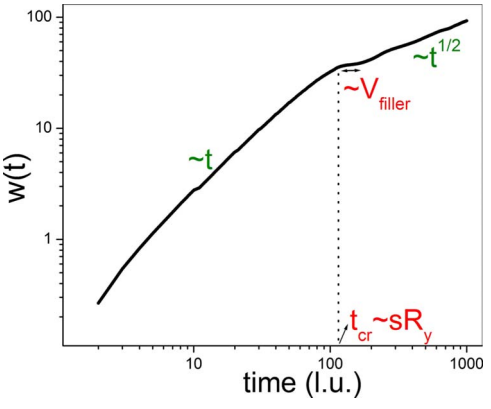

FIG. 12. (Color online) A typical time evolution of w of the surface of a composite film with $s=10$, $R_y=11$, and $V_{filler}=10\%$ during LLE.

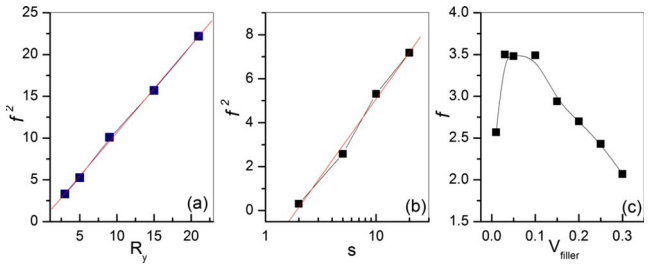

FIG. 13. (Color online) The dependencies of the prefactor f in $w(R,s,V_{\text{filler}};t)$ on (a) the filler vertical dimension R_y when $V_{\text{filler}}=10\%$, $s=10$, and $t=1000$; (b) the selectivity s when $V_{\text{filler}}=10\%$, $R_y=5$, and $t=1000$; and (c) the total filler volume V_{filler} with $s=10$, $R_y=11$, and $t=1000$. No effects of filler geometry on $w(t)$ have been noticed.

$$w(t;R_{x,y},V_{\text{filler}},s,\text{geometry}) = f(R_{x,y},V_{\text{filler}},s,\text{geometry})t^{1/2}.$$

Unfortunately, in the case of inhomogeneous films, no simple relation in analytical form can be extracted for f. Thus, the only way to determine the material parameter dependencies of f is the extensive and systematic numerical investigations whose results are shown in Fig. 13. Figure 13(a) indicates that, similarly to porous films, f depends only on the vertical dimension of fillers R_y and particularly $f\sim R_y^{1/2}$. The dependence on s is logarithmic $f\sim[\log(s)]^{1/2}$ as shown in Fig. 13(b), while the effect of total free volume is displayed in Fig. 13(c) and cannot be easily expressed in a closed form. Finally, fillers with various geometrical shapes have been inserted in the modeling of the film but no noticeable impact on $w(t)$ has been found.

B. Effects on $G(r,t)$

Figure 14(a) depicts the evolution of 1D surface during LLE of a composite film with fillers etched with smaller rate than bulk material. No specific features are developed on the surface besides the steep slopes, which become steeper as etching proceeds. The time dependence of the HHCF $G(r)$ is shown in Fig. 14(b). The behavior resembles closely that of

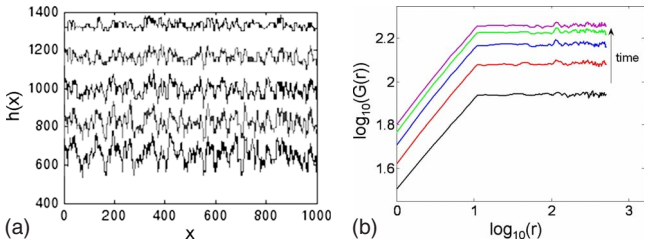

FIG. 14. (Color online) (a) The time evolution of the 1D surface of a composite film with fillers and (b) the time dependence of HHCF.

porous films. Thus the drawn conclusions are similar: fractal self-affine behavior for $r<\xi$ with $\xi=R_x$, where R_x is the horizontal dimension of the fillers, fixed correlation length vs time, sensitivity of roughness exponent on filler geometry and slightly on selectivity s, and, most importantly, anomalous scaling behavior belonging to the same universality class with the kinetic roughening of LLE of porous films.

VI. CONCLUSIONS

During the last 25 years we have witnessed the transfer of scaling concepts and methods from the study of critical phenomena in equilibrium phase transitions to nonequilibrium processes. A nonequilibrium physical phenomenon with both theoretical interest and technological relevance is roughness evolution during surface growth. Scaling methodology has been applied quite extensively in this process and quite early it was realized that a normal scaling behavior does not hold in a large number of experiments and models. The anomalous scaling kinetic roughening theory was envisaged to provide a comprehensive description of such roughness evolutions. However, the origins of the anomalous scaling remain largely unspecified.

In this paper, we used a simplified model (layer by layer removal of surface cells) for the etching of inhomogeneous films (porous and composites) in order to extract the effects of material inhomogeneities on roughness evolution, i.e., the roughness evolution $w(t)$ and the time dependence of height-height correlation function $G(r)$. Regarding the first quantity the following conclusions were reached:

(a) Randomly distributed material inhomogeneities (pores or fillers) lead to growth exponent $\beta=1/2$, i.e., $w(t)\sim t^{1/2}$.

(b) The size, total volume, and etch selectivity of inhomogeneities affect only the prefactor of the relation $w(R,V_{\text{filler}},s;t)=f(R,V_{\text{filler}},s)t^{1/2}$.

(c) Even slightly correlated inhomogeneities along etch direction lead to increase in growth exponent β.

Thus roughness evolution might be used as a diagnostic tool for the structure of inhomogeneous materials.

The investigation of the time evolution of the HHCF $G(r)$ during the LLE of inhomogeneous films showed that:

(a) Material inhomogeneities induce anomalous scaling behavior coupling with self-affine surface morphologies and roughness growth exponent $\beta=1/2$.

(b) The estimation of the critical scaling exponents shows that LLE induces another universality class characterized by fixed correlation length ($z=\infty$) and square-root time increase in surface width w ($\beta=1/2$).

Future work includes a more detailed modeling of the etching process and comparison with experimental results.

[1] A.-L. Barabasi and H. E. Stanley, *Fractal Concepts in Surface Growth* (Cambridge University Press, Cambridge, England, 1995).
[2] J. Krug, Adv. Phys. **46**, 139 (1997).
[3] R. Cuerno, M. Castro, J. M. García, R. Gago, and L. Vázquez, Eur. Phys. J. Spec. Top. **146**, 427 (2007).
[4] S. Facsko, T. Dekorsy, C. Koerdt, C. Trappe, H. Kurz, A. Vogt, and H. L. Hartnagel, Science **285**, 1551 (1999).
[5] E. Chason, T. M. Mayer, and A. Payne, Appl. Phys. Lett. **60**, 2353 (1992).
[6] G. Boulousis, V. Constantoudis, G. Kokkoris, and E. Gogolides, Nanotechnology **19**, 255301 (2008).
[7] G. Kokkoris, V. Constantoudis, P. Angelikopoulos, G. Boulousis, and E. Gogolides, Phys. Rev. B **76**, 193405 (2007).
[8] E. Gogolides, C. Boukouras, G. Kokkoris, O. Brain, A. Tserepi, and V. Constantoudis, Microelectron. Eng. **73-74**, 312 (2004).
[9] R. Petri, P. Brault, O. Vatel, D. Henry, E. Andre, P. Dumas, and F. Salvan, J. Appl. Phys. **75**, 7498 (1994).
[10] J. T. Drotar, Y.-P. Zhao, T.-M. Lu, and G.-C. Wang, Phys. Rev. B **61**, 3012 (2000).
[11] M. Martina and G. Cunge, J. Vac. Sci. Technol. B **26**, 1281 (2008).
[12] H. Tanaka, D. Cheng, M. Shikida, and K. Sato, Sens. Actuators, A **134**, 465 (2007).
[13] R. D. Mansano, P. Verdonck, and H. S. Maciel, Vacuum **48**, 677 (1997).
[14] Y. Osano and K. Ono, Jpn. J. Appl. Phys. **44**, 8650 (2005).
[15] S. W. Ong, E. S. Tok, and H. C. Kang, Phys. Rev. E **75**, 061607 (2007).
[16] E. S. Tok, S. W. Ong, and H. C. Kang, Phys. Rev. E **70**, 011604 (2004).
[17] U. Cvelbar, S. Pejovnik, M. Mozetie, and A. Zalar, Appl. Surf. Sci. **210**, 255 (2003).
[18] E. Zakka, V. Constantoudis, and E. Gogolides, IEEE Trans. Plasma Sci. **35**, 1359 (2007).
[19] F. Family and T. Vicsek, J. Phys. A **18**, L75 (1985).
[20] J. J. Ramasco, J. M. Lopez, and M. A. Rodriguez, Phys. Rev. Lett. **84**, 2199 (2000).
[21] J. M. Lopez, M. Castro, and R. Gallego, Phys. Rev. Lett. **94**, 166103 (2005).
[22] S. Yim, T. S. Jones, Phys. Rev. B **73**, 161305(R) (2006).
[23] M. A. Auger, L. Vázquez, R. Cuerno, M. Castro, M. Jergel, and O. Sánchez, Phys. Rev. B **73**, 045436 (2006).
[24] Y.-P. Zhao, G.-C. Wang, and T.-M. Lu, *Experimental Methods in the Physical Science Vol. 37* (Academic, New York 2001).
[25] W. M. Tong and R. W. Stanley, Annu. Rev. Phys. Chem. **45**, 401 (1994).
[26] D. Marton and J. Fine, Thin Solid Films **151**, 433 (1987).